Science of the Total Environment 878 (2023) 162917

Contents lists available at ScienceDirect

Science of the Total Environment

journal homepage: www.elsevier.com/locate/scitotenv

Land-use changes in Amazon and Atlantic rainforests modify organic matter and black carbon compositions transported from land to the coastal ocean

Tassiana Soares Gonçalves Serafim [a,*], Marcelo Gomes de Almeida [b], Gérard Thouzeau [c], Emma Michaud [c], Jutta Niggemann [d], Thorsten Dittmar [d,e], Michael Seidel [d], Carlos Eduardo de Rezende [b]

[a] Leibniz Institute for Baltic Sea Research Warnemünde, Seestrasse 15, 18119 Rostock, Germany
[b] Laboratório de Ciências Ambientais, Centro de Biociências e Biotecnologia, Universidade Estadual do Norte Fluminense Darcy Ribeiro, Campos dos Goytacazes RJ, CEP 28013-602, Brazil
[c] Univ Brest, CNRS, IRD, Ifremer, UMR 6539 - LEMAR, F-29280 Plouzané, France
[d] Research Group for Marine Geochemistry (ICBM-MPI Bridging Group), Institute for Chemistry and Biology of the Marine Environment, Carl von Ossietzky University Oldenburg, Germany
[e] Helmholtz Institute for Functional Marine Biodiversity (HIFMB) at the University of Oldenburg, Germany

HIGHLIGHTS

- Land-use changes modify the composition of the organic material transported by rivers from land to the coastal zone.
- Low black carbon content in Amazon coastal sediments is noted.
- Black carbon in mainly grass-covered drainage basins exhibit a higher condensation degree.

GRAPHICAL ABSTRACT

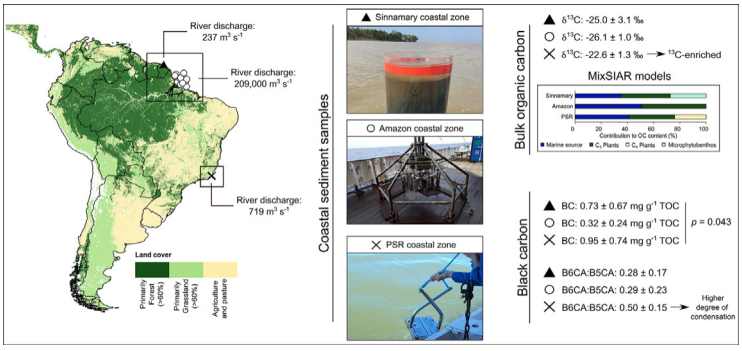

ARTICLE INFO

Editor: Ouyang Wei

Keywords:
Black carbon
Amazon rainforest
Atlantic rainforest
Carbon isotopic composition
Coastal sediments
Organic matter

ABSTRACT

This study assessed black carbon (BC) dynamics, concentrations, and the organic matter (OM) isotopic carbon composition in northeastern South America drainage basin coastal sediments. Paraíba do Sul (PSR; Atlantic Rainforest, Brazil) coastal sediments displayed more ^{13}C-enriched values (−22.6 ± 1.3 ‰ [n = 13]) than Amazon and Sinnamary (Amazon Rainforest in French Guiana and Brazil) sediments (−25.0 ± 3.1 ‰ [n = 14] and − 26.1 ± 1.0 ‰ [n = 6], respectively), indicating that local land-use basin changes have altered the OM composition, i.e., from natural C_3 plant to C_4 plants contributions. BC contents normalized to total organic carbon (TOC) content were 0.32 ± 0.24 (n = 8), 0.73 ± 0.67 (n = 6), and 0.95 ± 0.74 (n = 13) mg g^{-1} TOC for Amazon, Sinnamary and PSR samples, respectively, with BC sources appearing to differ according to different drainage basin vegetation covers. With increasing distance from the river mouths, BC contents exhibited different trends between the coastal zones, with values increasing for the PSR and decreasing values for the Amazon samples. BC distribution in Sinnamary coastal sediments did not display specific patterns. Regarding the Amazon coastal zone, BC contents decreased while the B6CA:B5CA ratios did not show a pattern, which could indicate that BC in the area originates from river transport (aged BC) and that the hydrophobic component of dissolved BC is removed. The BC content mostly increased in the PSR coastal zone, while the B6CA:B5CA ratios were not altered for the entire gradient, indicating the BC stability and possible atmospheric deposition of soot. Our findings indicate that different sources, transformation processes, and hydrological conditions affect BC contents within coastal zones. Continuous land cover changes in both the Amazon and Atlantic Rainforests may result in large-scale marine carbon cycling impacts.

* Corresponding author.
E-mail address: tassiana.sgs@gmail.com (T. Soares Gonçalves Serafim).

http://dx.doi.org/10.1016/j.scitotenv.2023.162917
Received 5 October 2022; Received in revised form 27 February 2023; Accepted 13 March 2023
Available online 17 March 2023

1. Introduction

The conversions of primary forest areas to croplands and agricultural areas have devastated the Brazilian Atlantic Rainforest, destroying important biomes such as the world's largest forest, the Amazon Rainforest (Ferrante and Fearnside, 2019), modifying organic matter (OM) soil contents (Bernardes et al., 2004). Native forest vegetation conversion has altered the Atlantic Rainforest landscape, with about 28 % of the original vegetation cover now distributed only in fragments (Rezende et al., 2018; Solórzano et al., 2021). Such anthropogenic areas currently comprise approximately 15 % of the entire Amazon biome (Stahl et al., 2016), and are now on the rise due to the destruction of forest areas. One strategy applied to forest biomass removal and the management of anthropogenic regions consists in fire cleaning (Edwards, 1984). Fire is currently considered the primary Amazon Rainforest biomass removal vector, through forest fires caused by drought events (Aragão et al., 2018) or anthropogenic activities, such as cattle pasture expansion and management and agricultural activities. Wildfires and anthropogenic burning globally emit about 2.2 Pg of carbon per year in the form of greenhouse gases (van der Werf et al., 2017). Furthermore, fires also produce another carbon-enriched form displaying higher resistance to degradation than non-thermally-altered OM, named black carbon (BC) (Forbes et al., 2006; Bird and Ascough, 2012).

Black carbon is commonly described as the thermally altered and condensed aromatic OM fraction produced after incomplete combustion of plant biomasses or fossil fuels (Goldberg, 1985). Hedges et al. (2000) described the broad spectrum of BC compounds as a combustion continuum, later termed the degradation continuum (Bird et al., 2015), ranging from levoglucosan to highly condensed aromatic compounds that may display environmental persistence (Wagner et al., 2021). The global production of BC derived from plant biomasses has been estimated as ranging between 50 and 300 Tg of BC per year (Forbes et al., 2006; Bird et al., 2015) and about 80 % of BC initially remains in BC production sites following combustion (Kuhlbusch and Crutzen, 1995). According to Reisser et al. (2016), BC comprises about 14 % of overall soil OM, with an average residence time of 88 years. This residence time, however, can range from a few years to millennia, depending on the combination of physical, chemical, and microbial processes (Singh et al., 2012). BC mobilization from soils and its entry into aquatic systems occurs mainly through the dissolved phase following solubilization of historical BC (Dittmar, 2008; Dittmar et al., 2012b) and lateral particle transport, mainly due to soil erosion (Major et al., 2010). In addition, BC inputs into aquatic systems can take place, to a smaller extent, via atmospheric transport, and its deposition can take place along the entire continent-ocean gradient (Jurado et al., 2008; Coppola et al., 2018).

Increased erosion due to land-use conversion increases particle transport into the aquatic system, resulting in the global accumulation of 75 Tg sediments per year, mainly in areas below 2000 m altitude (Wilkinson and McElroy, 2007). These eroded particles travel throughout the water column and eventually become deposited along the continent-ocean gradient, mainly in continental areas and transition zones, with only about 20 % of this suspended particulate matter (SPM) reaching their destination, the marine sediments (Bird et al., 2015; Coppola et al., 2018). The transport of SPM and associated OM along the continent gradient is influenced by river and drainage basin characteristics (Burdige, 2007). Suspended particulate matter transport is faster in small rivers usually associated with mountains, narrow continental shelves, or active continental margins, resulting in relatively low OM remineralization rates along the continent-ocean gradient (Blair et al., 2003). In contrast, SPM is subject to deposition and resuspension cycles in large rivers, resulting in increased OM remineralization due to long residence times (Aller, 1998). Additionally, OM (and BC) transported alongside particles can be replaced downstream by OM produced at lower elevations (Aller et al., 1996; Burdige, 2007).

By estimating BC contents associated with SPM and sediments of both large (e.g., the Amazon, Congo) and small (e.g., the Eel, Santa Clara, Danube) rivers, Coppola et al. (2018) reported that BC comprised about 15.8 ± 0.9 % of total organic carbon (TOC) content, and the data did not indicate associations between BC contents and river size. Furthermore, BC export dynamics in the rivers were attributed to soil erosion, where BC generally undergoes constant pre-ageing despite environmental conditions and settings. However, SPM transport to the ocean is considerably reduced due to strong physicochemical gradients, favoring certain processes, such as flocculation, in estuarine zones (Eisma, 1986). Regnier et al. (2013) estimated that about 20 % of the TOC associated with SPM does not reach the open ocean, due to deposition along continent–coastal gradients. The global flux of particulate BC to the ocean ranges from 19 to 80 Tg per year (Bird et al., 2015), assuming that BC comprises between 5 and 15 % of the TOC content (Cole et al., 2007). Lohmann et al. (2009) reported that BC accounted for between 3 and 35 % of OC contents in deep-sea sediments from the South Atlantic Ocean. These authors estimated the most recalcitrant form obtained by the degradation continuum model by isolating soot BC through the thermochemical oxidation technique and attributing its primary source as terrestrial by analyzing the isotopic organic carbon ($\delta^{13}C$) composition. To evaluate environmental BC sources, $\delta^{13}C$ values are often associated with BC content, as reported by Liu and Han (2021), who coupled BC content with $\delta^{13}C$ results and reported that the main source of BC associated to SPM in the Xijiang River Basin, in Southeast China, is fossil fuel combustion, accounting for around 80 % of the total BC content.

In this context, BC spatial dynamics and concentrations were assessed in the coastal sediments of three northeastern South American drainage basins. The Sinnamary (French Guiana) and Amazon River (Brazil) basins are covered by primary forest vegetation (terrestrial C_3 plants), whereas the Paraíba do Sul River (PSR; Brazil) basin is mainly covered with grasses (terrestrial C_4 plants), due to land-use changes. We further evaluated if the transition from primary forests to pasture and cultivation areas has altered the sources and composition of the OM deposited in associated coastal sediments. Black carbon content was analyzed by the benzene-polycarboxylic acid (BPCA) method, and elemental and isotopic OM compositions of bulk total organic carbon (TOC and $\delta^{13}C$), as well as nitrogen (N and $\delta^{15}N$) were determined. Three hypotheses were tested: (1) the OM of the PSR is ^{13}C-enriched compared to the Amazon River, due to vegetation basin cover alterations; (2) the BC content in the Amazon River coastal zone is lower compared to the other evaluated coastal sediments as a result of OM dilution and floodplain replacement; and (3) BC content is directly related to land use alterations in the PSR coastal zone and not to historical Atlantic Rainforest burning, as suggested previously for dissolved BC (Dittmar et al., 2012a, 2012b; Marques et al., 2017).

2. Material and methods

2.1. Study areas

2.1.1. The Amazon and French Guiana coastal zones

The Amazon Rainforest extends over several countries, including Brazil and French Guiana. Its surface area represents about 45 % of the world's remaining tropical forests (Laurance et al., 2001), which comprises approximately 4 % of the Earth's surface (about 6,100,000 km^2) (Malhi et al., 2008; Gallo and Vinzon, 2015). The Amazon Rainforest, besides playing an essential role in storing carbon in its biomass, is responsible for transporting terrestrial carbon to the Atlantic Ocean via the Amazon River (Cai et al., 1988; Malhi et al., 2006, 2008). The Amazon River exhibits a seasonal cycle with maximum discharge reaching an average of 209,000 $m^3\ s^{-1}$ from May to July (Latrubesse, 2008). Material discharges to the coastal zone comprise approximately 20 % of the global input of terrestrial material to the ocean (Richey et al., 1986; Ward et al., 2015). Due to the basin's climate, strong erosion and rapid particle deposition processes can lead to rapid sedimentation rate changes in the Amazon River plume area (Kuehl et al., 1986). The plume moves in a northwestern direction, and it has been suggested that a large portion of the OM in the sedimentary compartment of the Brazilian shelf and adjacent northwestern areas originates from the Amazon basin (Wells and Coleman, 1981; Nittrouer et al., 1986). Approximately 20 % of the SPM reaching the coastal zone is carried towards French Guiana,

due to interactions between the Brazilian North Current, east trade winds, and semi-diurnal sea currents (Geyer et al., 1996; Aller et al., 2004).

French Guiana vegetation cover comprises 97 % of tropical forest (Chave et al., 2001), with extensive mangrove forests covering over 80 % of the coast (Fromard et al., 2004). The Sinnamary River is considered a small river, and its drainage basin extends over 6565 km^2, with seasonal river discharges (Richard et al., 2000; Ray et al., 2018). The minimum and maximum discharge averages range between 193 and 700 m^3 s^{-1} in November (dry season) and June (wet season) 2015, respectively (Ray et al., 2018; source: DEAL GUYANE-EDF). According to Oliveira and Clavier (2000), water discharge variations in this area depends on the anthropogenic process of opening an upstream dam and the natural El Niño event. The Sinnamary River estuary undergoes a macro tidal regime, with a tidal range of ca. 3 m near the river mouth (Ray et al., 2018). The estuary's extensive mangrove forests are dominated by Avicennia germinans (Marchand et al., 2003; Marchand, 2017).

2.1.2. The Paraíba do Sul coastal zone

The Paraíba do Sul River (PSR) basin, comprising 57,000 km^2, extends over the states of São Paulo, Rio de Janeiro, and Minas Gerais in southeastern Brazil (Ovalle et al., 2013). The PSR occupies an area previously entirely covered by Atlantic Rainforest, and about 74 % of its basin is currently covered by pasture and sugar-cane crop areas (Figueiredo et al., 2011; Marques et al., 2017). Due to these changes, the basin has suffered from intense erosion, leading to higher particle inputs to the local aquatic system. The PSR estuary and the second largest mangrove forest in the state of Rio de Janeiro are located in São João da Barra, in the Norte Fluminense region (Bernini and Rezende, 2004). The PSR is a small- to a medium-sized river, whose discharges depend on the season. In the dry period, between June and September, PSR discharge rates vary between 200 and 500 m^3 s^{-1}, reaching a maximum of 2600 m^3 s^{-1} during the rainy period (Silva et al., 2001). The wet season of 2014 was atypical, due to low precipitation rates caused by sea level pressure anomalies in Southeastern Brazil, influenced by the La Niña event, causing extreme rain events.

2.2. Sampling

Surface sediment samples (0–2 cm) were obtained employing different techniques, totaling 33 samples distributed into six (hand core sampling), 14 (multicore sampler), and 13 (boxcore sampler) samples from the coastal Sinnamary River (5°21′ - 5°30′N and 52°56′ - 53°3′W), the Amazon River (2°S - 4°N and 46° - 51°W), and the PSR (21°28′ - 21°40′S and 40°48′ - 41°6′W) area, respectively (Fig. 1; Supplementary Table 1). Samples from the Sinnamary and PSR coastal zones were obtained near mangroves located in the intertidal estuarine zones, while Amazon samples were collected in the subtidal area under the influence of the Amazon plume. The sample sets were obtained during the wet season in January 2019, April 2018, and February 2014 at the Sinnamary, Amazon, and PSR coastal zones, respectively. The sediments were immediately frozen (−20 °C) after sampling until further analyses.

2.3. Elemental and isotopic organic matter compositions

Sediment samples were freeze-dried in the laboratory and homogenized. For the TOC and $\delta^{13}C$ determinations, samples (10 mg) were acidified in silver capsules for carbonate removal using 2 M HCl. For the N

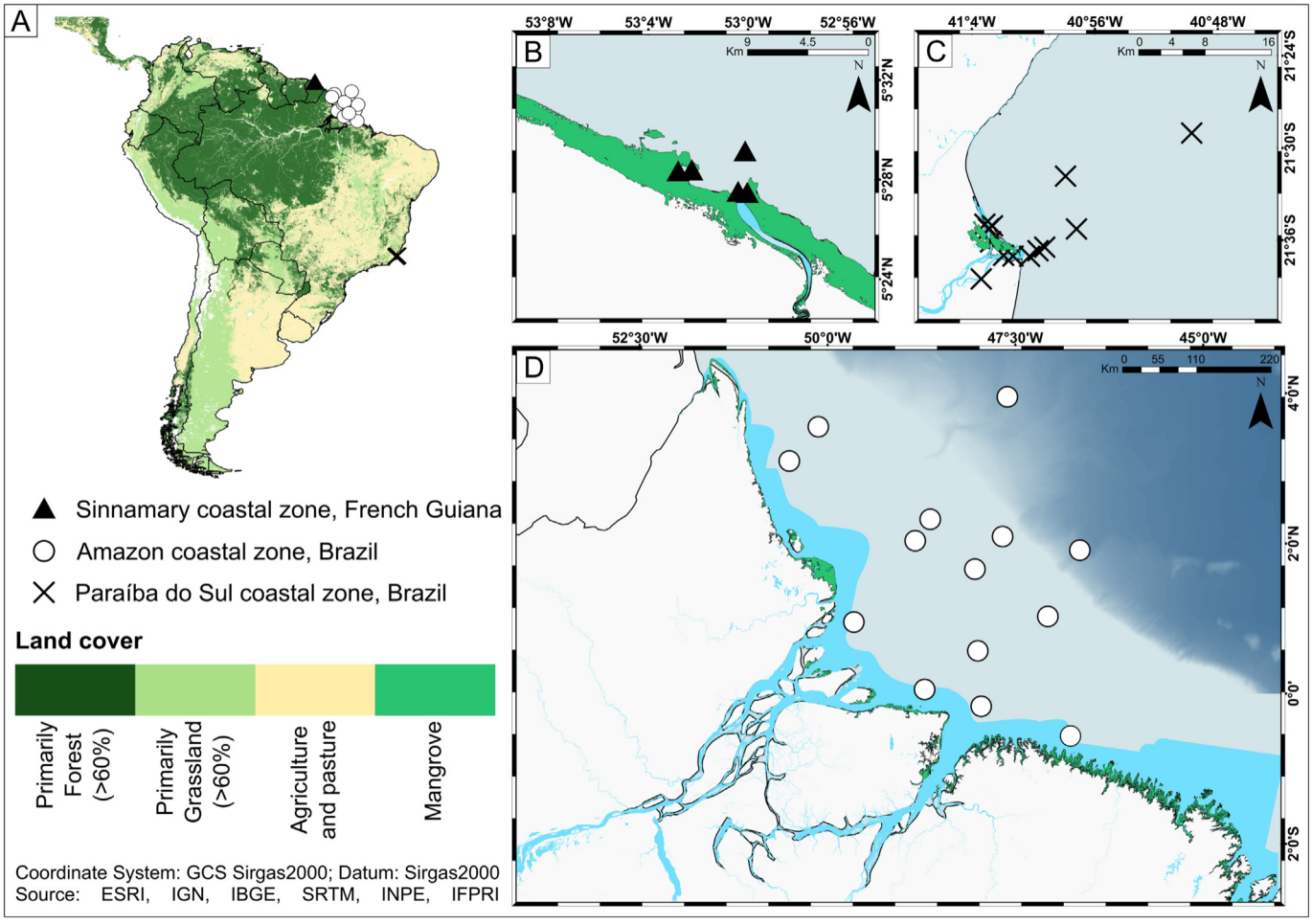

Fig. 1. South America sediment sampling sites: (A) the Sinnamary estuary, in the French Guiana (B), the Paraíba do Sul River estuary, in southeastern Brazil (C) and the Amazon plume, in northern Brazil (D).

and $\delta^{15}N$ determinations, samples (10 mg) were weighed into tin capsules. Elemental and isotopic values were obtained using a Flash 2000 elemental analyzer coupled to a Delta V mass spectrometer, with an uncertainty of measurement of 0.05 % for OC, 0.03 % for N, and ± 0.2 ‰ for $\delta^{15}N$ and $\delta^{13}C$.

2.4. Black carbon determination

BC contents were determined according to Glaser et al. (1998) and Brodowski et al. (2005) with slight adaptations. The samples were pre-digested with 10 mL trifluoroacetic acid for 4 h in a high-pressure system at 100 ± 5 °C, followed by filtering through GF/F filters (Whatman, pore size 0.7 μm). The filters were then placed in an oven for 2 h at 40 °C. After drying, 2 mL of nitric acid were added, and the samples were digested at 165 ± 5 °C for 8 h to obtain BPCAs from OM oxidation. The samples were again filtered through cellulose acetate filters (pore size 0.2 μm), and 8 mL of ultrapure water were added to dilute the applied nitric acid. A total of 50 μL of a surrogate (phthalic acid, 1 mg mL^{-1}) were added to 2.5 mL sample aliquots to correct for losses during the cleaning procedure, where the recovery was 60 ± 17 %, indicating sample losses during the process. Sample purification was conducted employing columns containing cation exchange resins after conditioning (Dowex 50 WX 8, 200–400 mesh, Fluka, Steinheim, Germany). The obtained sample volumes were separated into four vials and freeze-dried, resuspended with methanol and, finally, dried with N_2. The last sample cleaning step consisted in adding 4 mL of pyridine, a centrifugation step, and a new drying step with N_2. The samples were then analyzed by gas chromatography (GC–MS) and ultra-performance liquid chromatography (UPLC), according to Stubbins et al. (2015). The samples were derivatized for the GC–MS analysis using 250 μL of pyridine and 250 μL of N,O-bis (trimethylsilyl) trifluoroacetamide with 1 % trimethylchlorosilane (BSTFA-TMCS, 99:1) followed by heating for 2 h at 80 °C and then injected into the GC–MS. Biphenyl-2,2′-dicarboxylic acid was added as the internal standard before sample derivatization as an internal calibration of the GC–MS. Concerning the UPLC analysis, samples were dried with N_2 and resuspended in a phosphate buffer 100 μL (Na_2HPO_4 and NaH_2PO_4 each 5 mM in ultrapure water, pH 7.2).

The correction factor of 1.5 suggested by Schneider et al. (2011) was used for the samples analyzed via GC–MS to compare the data obtained by the different approaches since Schneider et al. (2011) reported analytical variability when comparing gas and liquid chromatography analyses. Other conversion factors reported for the BPCA method (i.e., Glaser et al., 1998) were not applied, as also suggested by Schneider et al. (2011). The standard reference sediment NIST 1941b was used to accurately and precisely determine BPCA contents. The mean BC content, normalized by the TOC content, detected by the GC–MS was 2.08 ± 0.17 mg g^{-1} TOC (n = 5), and the UPLC value was 2.97 ± 0.26 mg g^{-1} TOC (n = 3). The other two digestion products, B3CA and B4CA, were not assessed, as Kappenberg et al. (2016) demonstrated that these groups may be produced after the oxidation of non-pyrogenic OM, even when employing low sample weights (< 5 mg TOC). However, to allow for further comparisons, we also considered B3CA and B4CA with the conversion factor 2.27 from Glaser et al. (1998). Accordingly, the BC/TOC ratios and the BC contribution for the dry weight sediment found for NIST 1941b were 1.97 ± 0.48 and 0.05 ± 0.30 %, respectively, comparable to previously reported values by Hammes et al. (2007), with BC accounting for 0.06 ± 0.01 % of the dry sediment weight and BC/TOC ratios between 2.0 and 8.6.

2.5. Organic matter sources

Bayesian mixing models provide a synthesis of source and mixture data within a model structure that incorporates data variability (e.g., isotopic fractionation factor) (Parnell et al., 2010; Stock and Semmens, 2016), while linear mixing models consider that diagenetic changes do not significantly alter $\delta^{13}C$ and $\delta^{15}N$ OM values. Thus, the Bayesian MixSIAR mixing model was used to estimate the source contributions of each sample (Stock and Semmens, 2016; Stock et al., 2018). The MixSIAR applied Bayesian isotopic mixing and fitting models employing Markov chain Monte Carlo (MCMC) simulations of plausible values consistent with the dataset (n = 1,000,000, 100,000, and 1,000,000 for the Sinnamary, Amazon, and PSR coastal zones, respectively), with Gelman diagnostic variables lower than 1.05. Isotopic fractionation factors used for the models were calculated for each area and possible sources (Supplementary Table 2). The prior was set as "uninformative", where prior: α = c(1,1,1).

Two-endmember (Eq. (1)) (Shultz and Calder, 1976) and three-endmember linear models (Eq. (2)) (Fry, 2013) were used to evaluate the contributions of common terrestrial sources (terrestrial C_3 plants) for each sample to evaluate BC content associations:

$$C_3\ \text{plants} = \frac{\delta^{13}C_{Marine} - \delta^{13}C_{Sample}}{\delta^{13}C_{Marine} - \delta^{13}C_{Terrestrial}} \cdot 100 \quad (1)$$

where $\delta^{13}C_{Sample}$ is equivalent to the value found for a given sample, and $\delta^{13}C_{Terrestrial}$ and $\delta^{13}C_{Marine}$ are the isotopic composition values for terrestrial and marine sources, respectively. The assumed $\delta^{13}C$ value for the terrestrial C_3 plant endmember was −31.8 ‰ (Martinelli et al., 2021) versus −19.9 ‰ for the marine end-member (Bianchi et al., 2018) for the Amazon samples. As potential OM sources for the Sinnamary and PSR coastal zones are different, the model presenting the respective $\delta^{13}C$ and $\delta^{15}N$ values for each area was employed through the following Eq. (2):

$$C_3\ \text{plants} = \frac{(\delta^{15}N_C - \delta^{15}N_B)\cdot(\delta^{13}C_{Sample} - \delta^{13}C_B) - (\delta^{13}C_C - \delta^{13}C_B)\cdot(\delta^{15}N_{Sample} - \delta^{15}N_B)}{(\delta^{15}N_C - \delta^{15}N_B)\cdot(\delta^{13}C_A - \delta^{13}C_B - \delta^{13}C_C - \delta^{13}C_B)\cdot(\delta^{15}N_A - \delta^{15}N_B)} \quad (2)$$

where $\delta^{13}C_{Sample}$ and $\delta^{15}N_{Sample}$ comprise the isotopic composition values of the sediment samples. For the Sinnamary coastal zone, A, B, and C represent the OM sources originating from terrestrial C_3 plants (mangrove), microphytobenthos (MPB), and marine phytoplankton, respectively. The $\delta^{13}C$ and $\delta^{15}N$ values for the assessed mangrove (Avicennia germinans litter) were assumed to be −30.1 and 2.6 ‰, respectively, versus −20.9 and 4.6 ‰ for MPB (Ray et al., 2018). The marine source values during the wet season were − 23.9 and 3.4 ‰ for $\delta^{13}C$ and $\delta^{15}N$, respectively (Matos et al., 2020). Concerning the PSR coastal zone, the isotopic compositions of A, B, and C represent terrestrial C_3 plant, marine phytoplankton, and terrestrial C_4 plant sources, respectively. The $\delta^{13}C$ and $\delta^{15}N$ values for the terrestrial C_3 plant source were − 31.3 and 2.7 ‰, respectively (Martinelli et al., 2021). Concerning marine phytoplankton, $\delta^{13}C$ and $\delta^{15}N$ values were − 19.0 and 7.5 ‰, respectively (Gatts et al., 2020). The isotopic C and N values for terrestrial C_4 plants were − 14.6 ‰ (Ribas, 2012) and 7.1 ‰ (internal unpublished data), respectively.

The endmembers used for Eqs. (1) and (2) were the same as those employed for the Bayesian Mixing model, chosen based on literature values for each area, as different environmental settings can affect source isotopic compositions, such as latitude and altitude. The use of CO_2 by phytoplankton (considered as marine source) likely differs between the Sinnamary and Amazon coastal areas, due to distance from the coast, which could affect the isotopic compositions of the OM sources. Therefore, marine contributions for the Sinnamary coastal sediments were also considered, due to mangrove proximity.

2.6. Burial flux

The BC burial fluxes (F_{burial}) in coastal sediments were estimated through Eq. (3) (Sánchez-García et al., 2013):

$$F_{burial} = BC \cdot DBD \cdot SAR \quad (3)$$

where BC is the sum of B5CA and B6CA (μg g^{-1}), DBD is the dry bulk density (g cm^{-3}), and SAR is the sedimentation accumulation rate (cm yr^{-1}). The DBD values were calculated for each sample (Supplementary Table 3). SAR values were 0.74 (Allison and Lee, 2004) and 0.6

(Wanderley et al., 2013) for the Sinnamary and PSR coastal zones, respectively. The SAR values differed for the Amazon set sample (Supplementary Table 3), in agreement with Sobrinho et al. (2021), who grouped four different Amazon continental shelf regions presenting different deposition rates and sediment structures. Thus, SAR values differed among samples according to proximity to regions I, II and III (Supplementary Table 1). The central porosity value (0.75) commonly applied for global calculations was applied (Jönsson et al., 2003) to the Amazon and PSR coastal zones, while 0.5 was applied to the Sinnamary coastal zone, according to Aschenbroich et al. (2016).

2.7. Statistical analyses

Statistical analyses were performed using the R software (RC Team, 2018). Descriptive statistics comprising medians and interquartile ranges were employed. Differences in $\delta^{13}C$ (‰) values between the evaluated coastal zones were verified by the Kruskal Wallis test, while BC (mg g^{-1} TOC) and B6CA:B5CA contents were evaluated by an ANOVA test (aov, Base Package, RC Team, 2018) followed by a multiple comparison test (Tukey HSD, base package, RC Team, 2018) assuming a 95 % confidence level. Model assumptions (normality, linearity, and residual homoscedasticity) were tested by a maximum likelihood function (boxcox, MASS package, Venables and Ripley, 2002). If a transformation was indicated by the function, the correct adjustment was performed. The Pearson correlation analysis was performed to assess potential correlations between all analyzed parameters (e.g., distance from river mouths, $\delta^{13}C$, BC, contribution of terrestrial C_3 plant OM).

Furthermore, non-linear regression models were used to evaluate the associations and behaviors between $\delta^{13}C$, BC and the B6CA:B5CA ratios and river mouth distances (lm, Base Package, RC Team, 2018). Additionally, a linear model was constructed to assess associations between BC and the contribution of terrestrial C_3 plants to infer BC sources (lm, Base Package, RC Team, 2018). Model assumptions (normality, linearity, and residual homoscedasticity) were tested using a maximum likelihood function (boxcox, MASS package, Venables and Ripley, 2002); when a transformation was indicated by the function, the correct adjustment was applied.

3. Results

3.1. Organic matter sources

The $\delta^{13}C$ values from the coastal zone PSR OM were more ^{13}C-enriched (−22.6 ± 1.3 ‰, Kruskal-Wallis test $p < 0.01$) compared to the Sinnamary and Amazon River coastal sediments (−25.0 ± 3.1 and − 26.1 ± 1.0 ‰, respectively) (Fig. 2A; Supplementary Table 2). The $\delta^{13}C$ OM values ranged between −27.7 and − 25.1 ‰, −32.4 and − 20.7 ‰, and − 24.8 and − 20.4 ‰ for the Sinnamary, Amazon, and PSR coastal zones, respectively, with a trend towards ^{13}C enrichment with increasing distances from the Amazon and PSR river mouths (Fig. 2B).

The contribution of potential OM sources to the investigated sediment samples were determined by coupling $\delta^{13}C$ and $\delta^{15}N$ values (Fig. 3A). Bayesian stable isotope mixing models were used to determine OM sources (Fig. 3B). The estimated relative percentages of OM-contributing sources for Sinnamary River coastal sediments averaged 36.7, 26.4, and 37.0 % for marine sources, MPB, and terrestrial C_3 plants, respectively. Marine sources accounted for 48.7 % of the OM for Amazon coastal sediments, while terrestrial C_3 plants presented a significant contribution of 51.3 %. Contributions for PSR coastal sediments were 39.5 % marine, 35.6 % terrestrial C_3 plants, and 24.9 % terrestrial C_4 plants.

3.2. Black carbon in coastal zones

BC normalized by TOC content differed between the Amazon (0.32 ± 0.24 mg g^{-1} TOC) and PSR (0.95 ± 0.74 mg g^{-1} TOC) coastal zones (one-way ANOVA: $p = 0.035$), both of which exhibited similar concentrations to Sinnamary coastal sediments (0.73 ± 0.67 mg g^{-1} TOC; Fig. 4A). In addition, BC contents were moderately and positively correlated with TOC in the Sinnamary and Amazon coastal sediments ($r = 0.60$ and 0.66, respectively; Supplementary Fig. 1) and moderately and negatively correlated with TOC in PSR coastal sediments ($r = -0.60$; Supplementary Fig. 1). Concerning the PSR coastal zone, BC contents generally increased with river mouth distance, while a strong drop in BC contents was noted for both the Amazon and Sinnamary coastal sediments, with BC initially

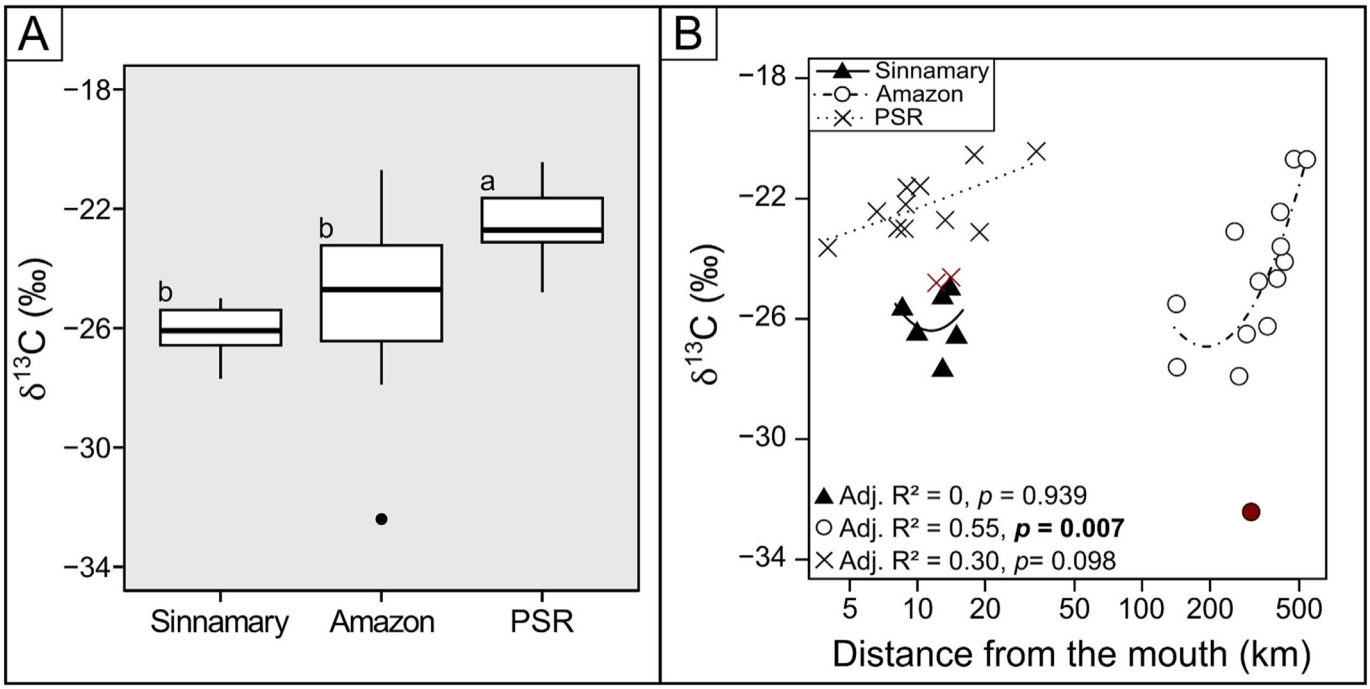

Fig. 2. Boxplots for $\delta^{13}C$ OM values (n = 6, 14 and 13, for Sinnamary, Amazon and PSR coastal zones, respectively) (A) and distribution according to river mouth distance (log km) (B). Different letters represent statistical significance for the difference in the means (Kruskal-Wallis tests, $p < 0.01$) and the circles represent outliers (A). Red symbol values were not used in model construction.

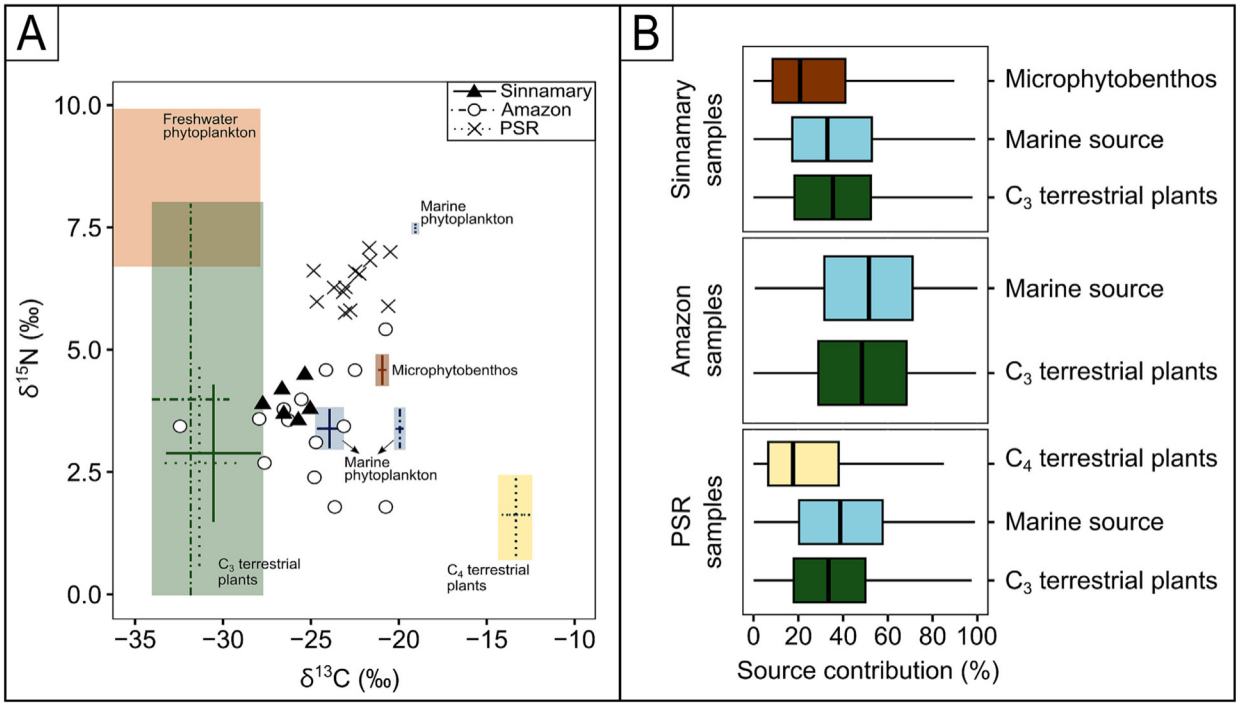

Fig. 3. Cross-plot of $\delta^{13}C$ vs $\delta^{15}N$ TOC and TN values. Polygons represent source material and lines represent the discrimination uncertainty (A). Relative contribution of the different sources for the investigated coastal zones (B). The $\delta^{13}C$ source material values were obtained from Ometto et al. (2006), Hamilton and Lewis (1992), Bouillon et al. (2011), Ray et al. (2018) and Ribas (2012). The $\delta^{15}N$ values were obtained from Ometto et al. (2006), Caraballo et al. (2014), Ray et al. (2018), and Ribas (2012).

increasing followed by a rapid drop associated to river mouth distance (Fig. 4C). The B6CA:B5CA ratios, used to assess BC degree of condensation, were highest in the PSR coastal zone samples (one-way ANOVA: $F = 4.826$, $p < 0.05$) compared to the other investigated coastal zones (Fig. 4B). The B6CA:B5CA ratios for the Sinnamary, Amazon, and PSR sediments were 0.28 ± 0.17, 0.29 ± 0.23, and 0.50 ± 0.15, respectively (Fig. 4B). The trends of the B6CA:B5CA ratios were not significant (Fig. 4D).

Potential BC sources for the investigated coastal zones were inferred employing the relationship between C_3 plant contributions (Eqs. (1) and (2)) and sedimentary OM and BC contents (Fig. 5). Black carbon contents increased with increasing C_3 plant OM contributions for the Sinnamary and Amazon coastal sediments, while the opposite was observed for the PSR.

The estimated BC burial fluxes were 2.19 ± 2.23, 0.13 ± 0.13 and 2.39 ± 1.50 μg cm^2 yr^{-1} for the Sinnamary, Amazon, and PSR coastal zones, respectively, with the lowest value observed for Amazon coastal zone.

4. Discussion

4.1. Organic matter coastal sediment sources reflect land-use changes

The detected ^{13}C enrichment of the PSR coastal sediments represents a typical signal of terrestrial C_3-C_4 plant mixtures, reflecting land-use changes in the PSR drainage basin (Fig. 2A). The enrichment of $\delta^{13}C$ values can be observed after decades of land-cover changes, decreasing from −25.1 to −20.2 ‰ in 50 years, as described by Vitorello et al. (1989). Ribas (2012) analyzed vegetation and soil $\delta^{13}C$ values in the PSR basin and reported that $\delta^{13}C$ soil and vegetation samples differed by around 5 ‰. The same trend was observed in forest areas, with more ^{13}C enriched soil values. As reported by Boschker and Middelburg (2002), the difference between forest vegetation and forest soils can be explained by the preferential use of ^{12}C compared to ^{13}C by microorganisms during OM soil mineralization (Blagodatskaya et al., 2011; Liu and Han, 2021), while different values for C_4 vegetation and soil can be explained by the land-use change. Concerning the PSR fluvial system, Marques (2017) reported ^{13}C-enriched values ranging from −25 to −23 ‰ for SPM, with C_4 plant contributions ranging from 27 to 40 % to particulate organic carbon, even after centuries of land-use change (Ribeiro et al., 2009). When reaching the aquatic system, the particulate organic carbon (POC) receives autochthonous material, such as from freshwater phytoplankton, with $\delta^{13}C$ values according to dissolved inorganic carbon in the water column used for photosynthesis (Vuorio et al., 2006). In the estuarine zone, POC $\delta^{13}C$ values observed by Marques (2017) were more ^{13}C depleted, ranging from −25.8 to −23.7 ‰, indicating mangrove contributions (terrestrial C_3 plants) that, in addition to autochthonous contributions, can dilute terrestrial C_4 plant contributions to coastal sediments. Indeed, according to the MixSIAR model, the terrestrial C_3 plant contribution to TOC content was higher than that of terrestrial C_4 plants (Fig. 3B), while marine production was the primary source for PSR coastal sediments. The marine source being so evident in the mixture of the MO can be attributed to low river discharge during the sampling period, to low precipitation rates, which were below 50 % of normally expected values due to a La Niña macroclimatic event (Marques et al., 2017) and to anthropogenic PSR watershed modifications (Carvalho et al., 2002; Souza et al., 2010).

Sedimentary OM in the Amazon and Sinnamary coastal zones exhibited a strong C_3 plant signal, as expected, since local rainforests are dominated by these types of plants (Figs. 1 and 2A). Therefore, the ^{13}C enrichment noted for Amazon coastal sediments highlights the increasing contribution of marine OM sources with increasing river mouth distances (Fig. 2B, Supplementary Fig. 1B). The determined sedimentary isotopic C and N composition indicates that marine sources contributed considerably to several surface sediment samples (Fig. 3A), in line with previous studies demonstrating that offshore TOC is mainly derived from marine primary production (Aller and Blair, 2006; Sobrinho et al., 2021). Ward et al. (2015) reported that about 50 % of continental OM does not reach the Amazon coastal zone due to intense OM river remineralization and sedimentation. In addition, according to Sobrinho et al. (2021), terrestrial OM that reaches the Amazon River delta comprises the main OM sediment source. Organic matter is, however, continuously remineralized in the Amazon River plume and terrestrial OM is replaced by marine OM, which explains the strong ^{13}C enrichment noted with increasing river mouth distances (Aller and Blair, 2006)

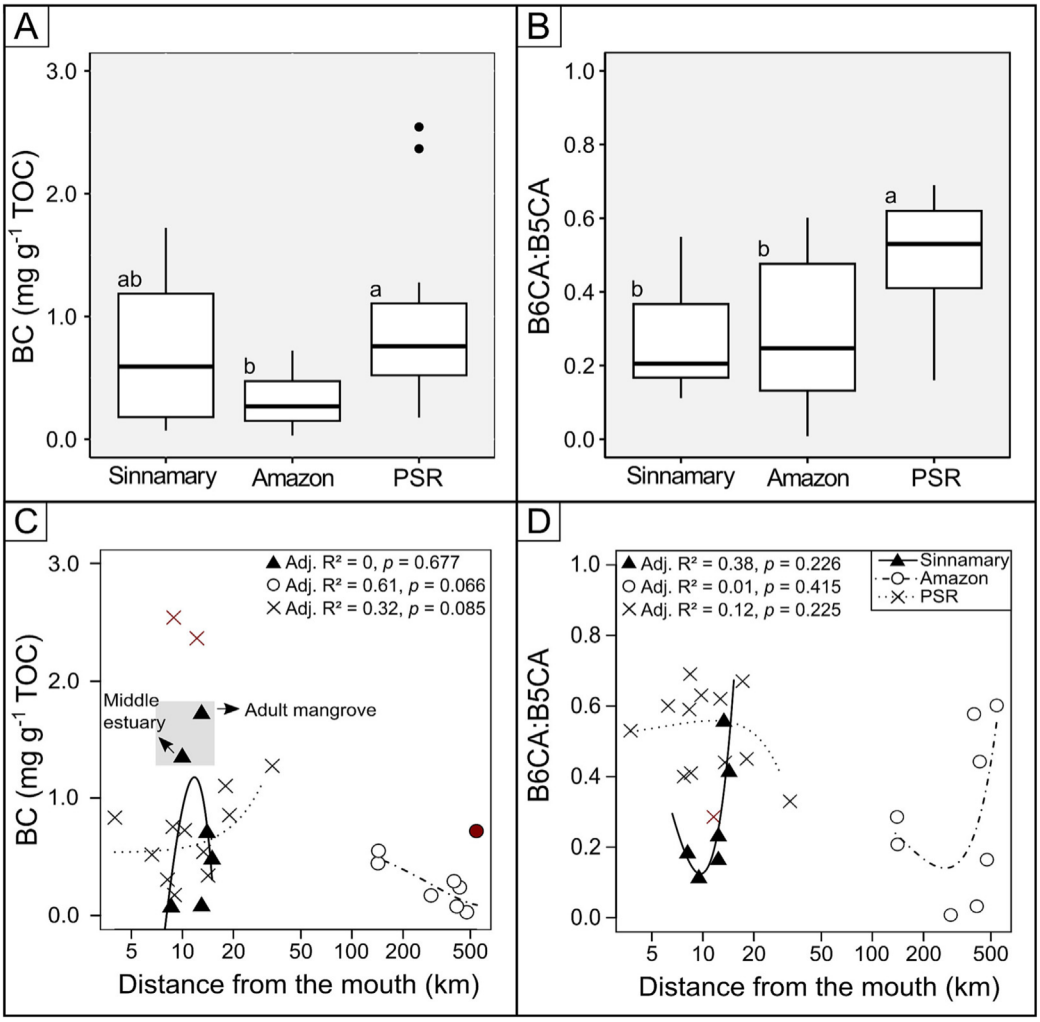

Fig. 4. Boxplots for BC values normalized to TOC content (A) and B6CA:B5CA ratios (B) (n = 6, 8 and 13, for Sinnamary, Amazon and PSR coastal zones, respectively). Relationship between BC content (C) and B6CA:B5CA ratios (D) concerning distance from the Sinnamary, Amazon, and PSR River mouths (log km). Letters represent the statistical significances for the differences in mean values (Tukey's test, $p < 0.05$), and circles represent outliers (A). Red symbols indicate values that were not used in model construction.

(Figs. 2B and 3B). This trend has also been reported by Sun et al. (2017), who detected ^{13}C-enriched isotopic values ranging from −21.4 and −23.0 ‰ in Amazon fan sediments. Additionally, by analyzing lignin phenols, these authors also demonstrated that terrestrial OM reaching the Amazon plume undergoes extensive diagenetic alterations before being deposited, as previously suggested by Aller and Blair (2006) and Ward et al. (2015).

Sinnamary coastal sediments exhibited a dominance of C_3 vegetation (e.g., from the extensive surrounding mangrove, river-transported debris, and autochthonous production) (Fig. 3). When investigating SPM at the Sinnamary estuary, Ray et al. (2018) reported the same OM source as that determined in the present study, also reporting significant contributions of the MPB biofilm to coastal sediments. In addition, a major contribution of terrestrial C_3 plants was noted by applying the equation model to determine the contribution for each sample, except for the sample collected near the pioneer mangrove area, where around 55 % of sediment OM originated from MPB. Conversely, the surface sediment sample from the adult mangrove area exhibited the lowest MPB contribution (14 %) and the highest terrestrial C_3 plant contribution (75 %). According to Marchand et al. (2003), the abundance of MPB biofilms decreases with increasing mangrove age due to decreased light availability caused by an increased canopy cover, hindering MPB photosynthesis. This ecological relationship explains the strong negative correlation observed herein between both sources ($r = -0.89$; Supplementary Fig. 1A).

4.2. Land use BC drivers in coastal zones

Sedimentary BC contents differed between the investigated coastal zones, with the Amazon presenting lower values (Fig. 4A). Indeed, no pyrogenic material was detected in six of the evaluated Amazon samples (Supplementary Table 1). The BPCA method includes the polycondensed aromatic BC fraction but does not detect labile pyrogenic molecules (Wagner et al., 2021) or the highly condensed fraction (Hammes et al., 2007). In addition, river mouth distance and river discharge likely play important roles in offshore BC transport. Less condensed pyrogenic material can be degraded in the fluvial portion of the land-ocean continuum, as turnover rates may range from days to weeks (Bird et al., 2015; Wagner et al., 2021). Therefore, the low BC content determined herein can be explained by dilution due to high river discharges. In addition, the high residence time of particles in river systems displaying extensive lowlands, such as the Amazon basin, can result in higher OM remineralization along the river system (Bianchi et al., 2018). Consequently, BC can be degraded and replaced by non-thermally modified OM in floodplains before reaching the coastal zone (Frueh et al., 2014; Cotrufo et al., 2016). This degradation in the river section of the land-ocean gradient may explain the low BC content, while the source change of TOC content (terrestrial to marine) explains the rapid BC content decline with increasing river mouth distance (Fig. 4A and C). The heterogeneity in the B6CA:B5CA ratios along the

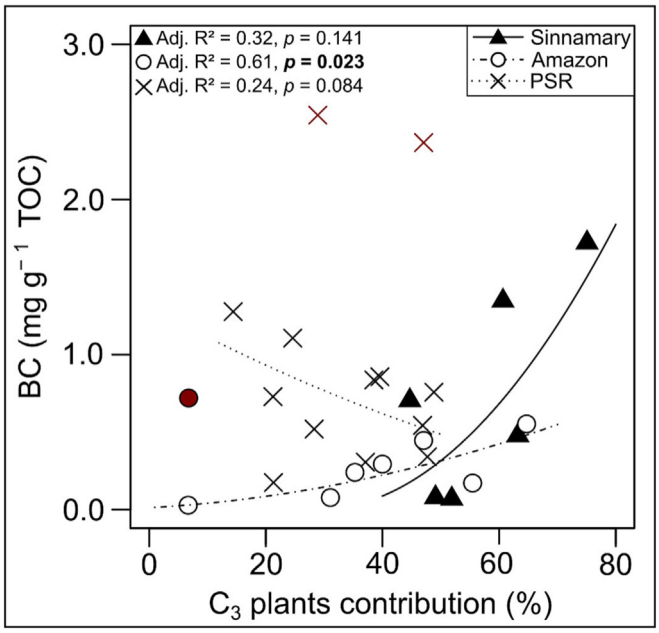

Fig. 5. Contribution of terrestrial C_3 plants to OM vs BC content in Sinnamary, Amazon, and PSR coastal zone sediments. Data points with red symbols were not used in model construction.

land-ocean gradient indicates the presence of two mechanisms acting on BC deposition in Amazon plume sediments, namely the removal of hydrophobic components from the dissolved BC fraction by co-precipitation (Coppola et al., 2014; Coppola et al., 2022), and the remobilization of aged BC from alluvial sedimentary deposits (Wagner et al., 2018). The first mechanism has been reported for the North Pacific Ocean, where dissolved BC contributes to sediment BC content through the adsorption of highly condensed structures (Nakane et al., 2017). This would explain why the sample with the highest BC content was the one obtained at the greatest distance to the river mouth. The second mechanism may be a consequence of energetic mixing and high particle load of the Amazon River, where particles are subject to numerous deposition and resuspension cycles during lateral transport. As a result, BC can be stored in intermediate reservoirs before being stored in marine sediments (McKee et al., 2004; Coppola et al., 2018).

Although the sedimentary BC contents at the Sinnamary River and PSR coastal zones were comparable, different trends were observed with increasing river mouth distances (Fig. 4A and C). In contrast to BC transport along the Amazon River land-ocean continuum, BC in small to medium-sized rivers such as the Sinnamary and PSR reaches the coastal zone faster due to the relatively short time between aquatic system entry and coastal sediment deposition (Burdige, 2007). Black carbon content seems to be heterogenous in the Sinnamary coastal zone, with a high BC contribution compared to TOC in two samples collected near the adult mangrove channel and in the middle estuary, where estuarine mixing takes place (Fig. 4C). Mangroves display a high allochthonous fluvial OM sediment retention capacity (Chew and Gallagher, 2018). Chew and Gallagher (2018) attributed the high BC to TOC ratio detected in mangrove sediments to fluvial BC transport, as mangroves rarely burn. Moreover, it is essential to highlight the importance of soot-derived BC canopy trapping (Agawin and Duarte, 2002; Chew and Gallagher, 2018). In the estuarine mixing zone, flocculation, and subsequent deposition facilitates the accumulation of fine particles, resulting in the deposition of thermally and non-thermally modified OM (Eisma et al., 1994). The removal of hydrophobic structures from dissolved BC may also explain the increasing B6CA:B5CA ratios of the sediment samples with increasing river mouth distance, also observed in the Amazon coastal sediments. The increasing B6CA:B5CA ratios with increasing distance from the Sinnamary river mouth can also be explained by atmospheric soot deposition since soot contains the most aromatic form of BC (Wolf et al., 2013; Saiz et al., 2015; Jones et al., 2017).

The BC content increased with increasing distance from the PSR mouth (Fig. 4C and Supplementary Fig. 1C), and the evaluated sediments exhibited higher BC condensation values (Fig. 4B), highlighting the refractory nature of BC in this coastal region. Saiz et al. (2015) observed a higher production of stable and refractory material in landscapes consisting mainly of grasses. The same trend observed by Wolf et al. (2013), with B6CA:B5CA ratios for forest and grass produced from immediate natural fires being 0.63 ± 0.12 and 0.99 ± 0.27, respectively. Thus, the current BC production in the PSR basin can explain the higher B6CA:B5CA ratios and the stability trend of thermally-modified OM along the land-ocean gradient. By applying the relationship between BC and the contribution of terrestrial C_4 plants, Marques et al. (2017) identified historical Atlantic Rainforest burning as the predominant source of dissolved BC in the PSR, as also suggested by Dittmar et al. (2012a), with B6CA:B5CA ratios ranging between 0.27 and 0.38. As mentioned previously, BC soil solubilization and its subsequent entry into the aquatic system can take decades (Dittmar et al., 2012b). It is therefore expected that BC originating from historical burning is mobilized from soils mainly by soil OM solubilization (Dittmar et al., 2012a). Changes in vegetation cover and current BC production increase soil erosion (Smith et al., 2011), making the input of particles into the aquatic system more significant for recently produced BC. When estimating BC content in SPM and dissolved OM, Wagner et al. (2015) reported an immediate BC contribution to SPM, with a decrease following the burning event, but increasing again during spring and late summer rain due to higher runoff. However, land-use fire management in pasture and sugarcane areas takes place annually in the PSR basin (Ferreira et al., 2021), continuously increasing the BC soil pool. Thus, the difference in BC sources and quality between the sediment compartments in the present study and the dissolved fraction in Marques et al. (2017) can be explained by differences in molecular composition modulation for the dissolved and particulate water fractions (Wagner et al., 2018).

4.3. BC sources and burial fluxes in coastal zones

The thermally modified OM in the sediment compartment of the evaluated coastal zones varied with the current vegetation cover of each basin (Fig. 5). However, the estimated contribution of C_3 plants does not distinguish vascular plants from autochthonous production in river waters, leading to a "mixture" factor in the determination coefficient. Historical Atlantic Rainforest burning explains the dissolved BC concentrations at the PSR (Marques et al., 2017), although sedimentary BC contents decreased with increasing terrestrial C_3 OM source contributions in PSR coastal sediments (Fig. 5). A high BC content (2.37 mg g^{-1} TOC) detected in one sample without contribution from terrestrial C_4 plants with a low B6CA:B5CA ratios may indicate the presence of old BC originating from historical Atlantic Rainforest burning or even from sugar cane fields that have been fire-managed for centuries in this area (Marques et al., 2017). Jones et al. (2017) highlighted the importance of atmospheric soot deposition for BC content in the PSR, indicating that recently produced soot (e.g., from biomass or fossil fuel burning) can be introduced into the water column after atmospheric deposition, being subsequently transported along with river SPM to be deposited in the coastal zone. Thus, in addition to riverine BC transport, BC can also originate from atmospheric deposition (Lara et al., 2005). In contrast, atmospheric transport to the Amazon and Sinnamary River mouths appears to not be significant concerning sedimentary BC contents. According to Coppola et al. (2019), BC originating from atmospheric deposition can be rapidly removed or diluted in the fluvial sector of the Amazon River. In the PSR coastal zone however, a constant BC supply to the coastal zone is directly linked to the annual fire management of croplands and pasture areas.

Black carbon burial flux estimates for coastal zones are important to better understand the role of thermally modified OM in the global carbon cycle, as burial in coastal sediments is an essential BC sink (Sánchez-García et al., 2013; Bird et al., 2015). The burial flux observed

for the Amazon coastal zone was significantly lower compared to the other investigated coastal zones (one-way ANOVA: $p < 0.001$) and was strongly and negatively correlated with increasing river mouth distance ($r = -0.88$). Similarly, no differences between the Sinnamary and PSR coastal zones were observed. Including the B3CA and B4CA markers increased the burial flux for PSR coastal to values between 2.61 and 306.19 μg cm^{-2} y^{-1}, which is, for example, lower than the burial flux reported by Sánchez-García et al. (2013) in the Gulf of Cádiz, Spain. However, since different BC determination methods along the combustion continuum are available (e.g., including B3CA and B4CA in BC content estimates and/or applying conversion factors [Glaser et al., 1998]), BC data derived from different analytical techniques should be compared cautiously (Masiello, 2004; Schneider et al., 2011; Kappenberg et al., 2016).

Black carbon contents can also be associated to organic and inorganic pollutants (Nam et al., 2008; Lian and Xing, 2017). For example, Neupane et al. (2020) reported a positive correlation between BC contents (mainly produced by biomass burning) and Hg concentrations ($R^2 = 0.48$, $p < 0.001$), suggesting similar sources and/or transport mechanisms in Selin Co lake surface sediments, located in the central Tibetan Plateau. At the PSR coastal zone, the constant BC input to the coastal zone is most likely directly associated to the annual management of croplands and pasture areas (Ferreira et al., 2021) while Hg is used in the sugar-cane management against pests (Câmara et al., 1986). Therefore, Hg can be released to the atmosphere by soil volatilization during the fire management of croplands and pasture areas and, alongside BC, is transported to aquatic systems, either by fluvial or atmospheric transport. Moreover, Nam et al. (2008) reported a correlation between BC and persistent organic pollutants, although they emphasized that this relationship could be masked by the old BC soil stocks. Consequently, understanding BC transport and burial fluxes will aid in elucidating carbon sinks and also the fate of contaminants in coastal sediments, especially considering that BC exhibits environmental persistence.

5. Conclusions

In the present study, $\delta^{13}C$ coupled with $\delta^{15}N$ analyses and mixing models were employed to understand the sources, composition, and spatial dynamics of the organic matter in coastal sediments in northeastern South American coastal zones in Brazil and French Guiana. Altered vegetation covers from forests to grasslands were indicated as an OM modification driver in the investigated coastal sediments. Additionally, we analyzed the contribution of terrestrial OM (C_3 plants) to understand BC sources in the assessed drainage basins. In PSR coastal sediments, a mixture of ^{13}C-enriched OM derived from C_3 and C_4 plants, demonstrated that human-induced modifications from Atlantic Rainforest to croplands and pasture areas altered the OM composition transported to the coastal zone. Concerning the BC source for this drainage basin, we suggest that BC produced from the incomplete burning of terrestrial C_4 plant biomass is the main BC source for PSR coastal sediments (Fig. 5; Supplementary Fig. 1), even though the $\delta^{13}C$ analysis was performed on bulk TOC and not directly on molecular BC markers (BPCA).

Remineralization and sedimentation processes along the land-ocean continuum of the Amazon River coupled to high river discharges can explain the lower BC contents detected in the Amazon coastal zone compared to the PSR and Sinnamary study sites. However, this could change in the future due to the high agricultural expansion noted in the Amazon, which could exacerbate social and ecological impacts in this biome. Over the past 14 years, deforestation and forest fire rates in the Amazon have reached record levels, with anthropogenic activities increasingly removing Amazon Rainforest biomass, resulting in increased BC contents in soil and BC transported to the coastal zone. Even though land-use changes display the potential to produce more stable BC, it is crucial to consider that the Amazon rainforest accounts for 93 ± 23 Pg C stored aboveground, which can substantially increase BC production and lead to significant carbon cycle impacts.

Supplementary data to this article can be found online at https://doi.org/10.1016/j.scitotenv.2023.162917.

CRediT authorship contribution statement

Tassiana S.G. Serafim: Conceptualization, Methodology, Investigation, Visualization, Writing – original draft, Writing – review & editing. Marcelo G. Almeida: Methodology. Gérard Thouzeau: Methodology, Writing – review & editing. Emma Michaud: Funding acquisition, Writing – review & editing. Jutta Niggemann: Writing – review & editing. Thorsten Dittmar: Funding acquisition, Writing – review & editing. Michael Seidel: Writing – review & editing. Carlos E. Rezende: Conceptualization, Funding acquisition, Project administration, Supervision, Writing – review & editing.

Data availability

Data will be made available on request.

Declaration of competing interest

The authors declare that they have no known competing financial interests or personal relationships that could have appeared to influence the work reported in this paper.

Acknowledgments

Research in the French Guiana was co-funded by the French National Agency under the programs "Investissements d'Avenir" (LabexMER: ANR-10-LABX-19), by the CNRS MITI program ("Pépinière Interdisciplinaire de Guyane") and by the French Research Institute for Sustainable Development (IRD). The International GEOTRACES Programme and support from the U.S. National Science Foundation (Grant OCE-1840868) to the Scientific Committee on Oceanic Research (SCOR) are also acknowledged. The German Science Foundation (DFG) is acknowledged for funding the R/V Meteor cruise M147. C.E. Rezende received financial support from CNPq (305217/2017-8) and FAPERJ (E-26/010.001272/2016 and E-26/200.893/2021), and this publication is part of his contribution to the INCT TMCOcean on material transfer at the land-ocean interace. T. S. G. Serafim is grateful for the Master's fellowship from CAPES (88887.46522/2019) and to FAPERJ for the training and technical qualification fellowship (E-26/203.884/2021), as well to Heike Simon for all the support during the BPCA analysis at the Institute for Chemistry and Biology of the Marine Environment. This research is a GDR LIGA contribution.

References

Agawin, N.S.R., Duarte, C.M., 2002. Evidence of direct particle trapping by a tropical seagrass meadow. Estuaries https://doi.org/10.1007/bf02692217.

Aller, R.C., 1998. Mobile deltaic and continental shelf muds as suboxic, fluidized bed reactors. Mar. Chem. https://doi.org/10.1016/s0304-4203(98)00024-3.

Aller, R.C., Blair, N.E., 2006. Carbon remineralization in the Amazon-Guianas tropical mobile mudbelt: a sedimentary incinerator. Cont. Shelf Res. https://doi.org/10.1016/j.csr.2006.07.016.

Aller, R.C., Blair, N.E., Xia, Q., Rude, P.D., 1996. Remineralization rates, recycling, and storage of carbon in Amazon shelf sediments. Cont. Shelf Res. https://doi.org/10.1016/0278-4343(95)00046-1.

Aller, R.C., Heilbrun, C., Panzeca, C., Zhu, Z., Baltzer, F., 2004. Coupling between sedimentary dynamics, early diagenetic processes, and biogeochemical cycling in the Amazon-Guianas mobile mud belt: coastal French Guiana. Mar. Geol. https://doi.org/10.1016/j.margeo.2004.04.027.

Allison, M.A., Lee, M.T., 2004. Sediment exchange between Amazon mudbanks and shore-fringing mangroves in French Guiana. Mar. Geol. https://doi.org/10.1016/j.margeo.2004.04.026.

Aragão, L.E.O.C., Anderson, L.O., Fonseca, M.G., Rosan, T.M., Vedovato, L.B., Wagner, F.H., Silva, C.V.J., Silva Junior, C.H.L., Arai, E., Aguiar, A.P., Barlow, J., Berenguer, E., Deeter, M.N., Domingues, L.G., Gatti, L., Gloor, M., Malhi, Y., Marengo, J.A., Miller, J.B., Phillips, O.L., Saatchi, S., 2018. 21st century drought-related fires counteract the decline of Amazon deforestation carbon emissions. Nat.Commun. https://doi.org/10.1038/s41467-017-02771-y.

Aschenbroich, A., Michaud, E., Stieglitz, T., Fromard, F., Gardel, A., Tavares, M., Thouzeau, G., 2016. Brachyuran crab community structure and associated sediment reworking activities in pioneer and young mangroves of French Guiana, South America. Estuar. Coast.Shelf Sci. 182, 60–71. https://doi.org/10.1016/j.ecss.2016.09.003.

Bernardes, M.C., Martinelli, L.A., Krusche, A.V., Gudeman, J., Moreira, M., Victoria, R.L., Ometto, J.P.H., Ballester, M.V.R., Aufdenkampe, A.K., Richey, J.E., Hedges, J.I., 2004.

Riverine organic matter composition as a function of land use change, Southwest Amazon. Ecol. Applic. https://doi.org/10.1890/01-6028.
Bernini, E., Rezende, C.E., 2004. Estrutura da vegetação em florestas de mangue do estuário do rio Paraíba do Sul, Estado do Rio de Janeiro, Brasil. Acta Bot. Bras. https://doi.org/10.1590/s0102-33062004000300009.
Bianchi, T.S., Cui, X., Blair, N.E., Burdige, D.J., Eglinton, T.I., Galy, V., 2018. Centers of organic carbon burial and oxidation at the land-ocean interface. Org. Geochem. https://doi.org/10.1016/j.orggeochem.2017.09.008.
Bird, M.I., Ascough, P.L., 2012. Isotopes in pyrogenic carbon: a review. Org. Geochem. https://doi.org/10.1016/j.orggeochem.2010.09.005.
Bird, M.I., Wynn, J.G., Saiz, G., Wurster, C.M., McBeath, A., 2015. The pyrogenic carbon cycle. Annu. Rev. Earth Planet. Sci. https://doi.org/10.1146/annurev-earth-060614-105038.
Blagodatskaya, E., Yuyukina, T., Blagodatsky, S., Kuzyakov, Y., 2011. Turnover of soil organic matter and of microbial biomass under C3–C4 vegetation change: consideration of 13C fractionation and preferential substrate utilization. Soil Biol. Biochem. https://doi.org/10.1016/j.soilbio.2010.09.028.
Blair, N.E., Leithold, E.L., Ford, S.T., Peeler, K.A., Holmes, J.C., Perkey, D.W., 2003. The persistence of memory: the fate of ancient sedimentary organic carbon in a modern sedimentary system. Geochim. Cosmochim. Acta https://doi.org/10.1016/s0016-7037(02)01043-8.
Boschker, H.T.S., Middelburg, J.J., 2002. Stable isotopes and biomarkers in microbial ecology. FEMS Microbiol. Ecol. https://doi.org/10.1111/j.1574-6941.2002.tb00940.x.
Bouillon, S., Connolly, R.M., Gillikin, D.P., 2011. Use of stable isotopes to understand food webs and ecosystem functioning in estuaries. Treatise on Estuarine And Coastal Science https://doi.org/10.1016/b978-0-12-374711-2.00711-7.
Brodowski, S., Rodionov, A., Haumaier, L., Glaser, B., Amelung, W., 2005. Revised black carbon assessment using benzene polycarboxylic acids. Org. Geochem. https://doi.org/10.1016/j.orggeochem.2005.03.011.
Burdige, D.J., 2007. Preservation of organic matter in marine sediments: controls, mechanisms, and an imbalance in sediment organic carbon budgets? ChemInform https://doi.org/10.1002/chin.200720266.
Cai, D.-L., Tan, F.C., Edmond, J.M., 1988. Sources and transport of particulate organic carbon in the Amazon River and estuary. Estuar. Coast. Shelf Sci. https://doi.org/10.1016/0272-7714(88)90008-x.
Câmara, V.de M., de M. Câmara, V., Campos, R.C., Perez, M.A., Tambelini, A.T., Klein, C.H., 1986. Teores de mercúrio no cabelo: um estudo comparativo em trabalhadores da lavoura de cana-de-açúcar com exposição pregressa aos fungicidas organo-mercuriais no município de Campos - RJ. Cad. Saúde Pública https://doi.org/10.1590/s0102-311x1986000300008.
Caraballo, P., Forsberg, B.R., de Almeida, F.F., Leite, R.G., 2014. Diel patterns of temperature, conductivity and dissolved oxygen in an Amazon floodplain lake: description of a friagem phenomenon. Acta Limnol.Bras. https://doi.org/10.1590/s2179-975x2014000300011.
Carvalho, C.E.V., Salomão, M.S.M., Molisani, M.M., Rezende, C.E., Lacerda, L.D., 2002. Contribution of a medium-sized tropical river to the particulate heavy-metal load for the South Atlantic Ocean. Sci. Total Environ. https://doi.org/10.1016/s0048-9697(01)00869-5.
Chave, J., Riéra, B., Dubois, M.-A., 2001. Estimation of biomass in a neotropical forest of French Guiana: spatial and temporal variability. J. Trop. Ecol. https://doi.org/10.1017/s0266467401001055.
Chew, S.T., Gallagher, J.B., 2018. Accounting for black carbon lowers estimates of blue carbon storage services. Sci. Rep. 8, 2553. https://doi.org/10.1038/s41598-018-20644-2.
Cole, J.J., Prairie, Y.T., Caraco, N.F., McDowell, W.H., Tranvik, L.J., Striegl, R.G., Duarte, C.M., Kortelainen, P., Downing, J.A., Middelburg, J.J., Melack, J., 2007. Plumbing the global carbon cycle: integrating inland waters into the terrestrial carbon budget. Ecosystems https://doi.org/10.1007/s10021-006-9013-8.
Coppola, A.I., Ziolkowski, L.A., Masiello, C.A., Druffel, E.R.M., 2014. Aged black carbon in marine sediments and sinking particles. Geophys. Res. Lett. https://doi.org/10.1002/2013gl059068.
Coppola, A.I., Wiedemeier, D.B., Galy, V., Haghipour, N., Hanke, U.M., Nascimento, G.S., Usman, M., Blattmann, T.M., Reisser, M., Freymond, C.V., Zhao, M., Voss, B., Wacker, L., Schefuß, E., Peucker-Ehrenbrink, B., Abiven, S., Schmidt, M.W.I., Eglinton, T.I., 2018. Publisher correction: global-scale evidence for the refractory nature of riverine black carbon. Nat. Geosci. https://doi.org/10.1038/s41561-018-0252-z.
Coppola, A.I., Seidel, M., Ward, N.D., Viviroli, D., Nascimento, G.S., Haghipour, N., Revels, B.N., Abiven, S., Jones, M.W., Richey, J.E., Eglinton, T.I., Dittmar, T., Schmidt, M.W.I., 2019. Marked isotopic variability within and between the Amazon River and marine dissolved black carbon pools. Nat. Commun. https://doi.org/10.1038/s41467-019-11543-9.
Coppola, A.I., Wagner, S., Lennartz, S.T., Seidel, M., Ward, N.D., Dittmar, T., Santín, C., Jones, M.W., 2022. The black carbon cycle and its role in the Earth system. Nat.Rev. EarthEnviron. https://doi.org/10.1038/s43017-022-00316-6.
Cotrufo, M.F., Francesca Cotrufo, M., Boot, C.M., Kampf, S., Nelson, P.A., Brogan, D.J., Covino, T., Haddix, M.L., MacDonald, L.H., Rathburn, S., Ryan-Bukett, S., Schmeer, S., Hall, E., 2016. Redistribution of pyrogenic carbon from hillslopes to stream corridors following a large montane wildfire. Glob. Biogeochem. Cycles https://doi.org/10.1002/2016gb005467.
Dittmar, T., 2008. The molecular level determination of black carbon in marine dissolved organic matter. Org. Geochem. https://doi.org/10.1016/j.orggeochem.2008.01.015.
Dittmar, T., de Rezende, C.E., Manecki, M., Niggemann, J., Ovalle, A.R.C., Stubbins, A., Bernardes, M.C., 2012a. Continuous flux of dissolved black carbon from a vanished tropical forest biome. Nat. Geosci. https://doi.org/10.1038/ngeo1541.
Dittmar, T., Paeng, J., Gihring, T.M., Suryaputra, I.G.N., Huettel, M., 2012b. Discharge of dissolved black carbon from a fire-affected intertidal system. Limnol. Oceanogr. https://doi.org/10.4319/lo.2012.57.4.1171.
Edwards, P.J., 1984. The use of fire as a management tool. Ecol.Stud. https://doi.org/10.1007/978-3-642-69805-7_16.
Eisma, D., 1986. Flocculation and de-flocculation of suspended matter in estuaries. Neth. J. Sea Res. https://doi.org/10.1016/0077-7579(86)90041-4.
Eisma, D., Chen, S., Li, A., 1994. Tidal variations in suspended matter floc size in the Elbe river and Dollard estuaries. Neth. J. Aquat. Ecol. https://doi.org/10.1007/bf02334194.
Ferrante, L., Fearnside, P.M., 2019. Brazil's new president and "ruralists" threaten Amazonia's environment, traditional peoples and the global climate. Environ. Conserv. https://doi.org/10.1017/s0376892919000213.
Ferreira, R., Nunes, C., Souza, M., Canela, M., 2021. Multivariate optimization of extraction variables of PAH in particulate matter (PM10) in indoor/outdoor air at Campos dos Goytacazes,Brazil. J. Braz. Chem. Soc. https://doi.org/10.21577/0103-5053.20200216.
Figueiredo, R.de O., de Oliveira Figueiredo, R., Ovalle, A.R.C., de Rezende, C.E., Martinelli, L.A., 2011. Carbon and nitrogen in the Lower Basin of the Paraíba do Sul River, Southeastern Brazil: element fluxes and biogeochemical processes. Ambiente Agua https://doi.org/10.4136/ambi-agua.183.
Forbes, M.S., Raison, R.J., Skjemstad, J.O., 2006. Formation, transformation and transport of black carbon (charcoal) in terrestrial and aquatic ecosystems. Sci. Total Environ. 370, 190–206. https://doi.org/10.1016/j.scitotenv.2006.06.007.
Fromard, F., Vega, C., Proisy, C., 2004. Half a century of dynamic coastal change affecting mangrove shorelines of French Guiana. A case study based on remote sensing data analyses and field surveys. Mar.Geol. https://doi.org/10.1016/j.margeo.2004.04.018.
Frueh, W.T., Terry Frueh, W., Lancaster, S.T., 2014. Correction of deposit ages for inherited ages of charcoal: implications for sediment dynamics inferred from random sampling of deposits on headwater valley floors. Quat. Sci. Rev. https://doi.org/10.1016/j.quascirev.2013.10.029.
Fry, B., 2013. Alternative approaches for solving underdetermined isotope mixing problems. Mar. Ecol. Prog. Ser. https://doi.org/10.3354/meps10168.
Gallo, M.N., Vinzon, S.B., 2015. Estudo numérico do escoamento em planícies de marés do canal Norte (estuário do rio Amazonas). Ribagua https://doi.org/10.1016/j.riba.2015.04.002.
Gatts, P.V., Franco, M.A.L., Almeida, M.G., Zalmon, I.R., Di Beneditto, A.P.M., Costa, P.A.S., de Rezende, C.E., 2020. The trophic ecology of marine catfishes in south-eastern Brazil. J. Mar. Biol. Assoc. U. K. https://doi.org/10.1017/s0025315419001164.
Geyer, W.R., Rockwell Geyer, W., Beardsley, R.C., Lentz, S.J., Candela, J., Limeburner, R., Johns, W.E., Castro, B.M., Soares, I.D., 1996. Physical oceanography of the Amazon shelf. Cont. Shelf Res. https://doi.org/10.1016/0278-4343(95)00051-8.
Glaser, B., Haumaier, L., Guggenberger, G., Zech, W., 1998. Black carbon in soils: the use of benzenecarboxylic acids as specific markers. Org. Geochem. https://doi.org/10.1016/s0146-6380(98)00194-6.
Goldberg, E.D., 1985. Black Carbon in the Environment: Properties And Distribution. John Wiley and Sons 1985.
Hamilton, S.K., Lewis, W.M., 1992. Stable carbon and nitrogen isotopes in algae and detritus from the Orinoco River floodplain, Venezuela. Geochim. Cosmochim. Acta https://doi.org/10.1016/0016-7037(92)90264-j.
Hammes, K., Schmidt, M.W.I., Smernik, R.J., Currie, L.A., Ball, W.P., Nguyen, T.H., Louchouarn, P., Houel, S., Gustafsson, Ö., Elmquist, M., Cornelissen, G., Skjemstad, J.O., Masiello, C.A., Song, J., Peng, P.'an, Mitra, S., Dunn, J.C., Hatcher, P.G., Hockaday, W.C., Smith, D.M., Hartkopf-Fröder, C., Böhmer, A., Lüer, B., Huebert, B.J., Amelung, W., Brodowski, S., Huang, L., Zhang, W., Gschwend, P.M., Xanat Flores-Cervantes, D., Largeau, C., Rouzaud, J.-N., Rumpel, C., Guggenberger, G., Kaiser, K., Rodionov, A., Gonzalez-Vila, F.J., Gonzalez-Perez, J.A., de la Rosa, J.M., Manning, D.A.C., López-Capél, E., Ding, L., 2007. Comparison of quantification methods to measure fire-derived (black/elemental) carbon in soils and sediments using reference materials from soil, water, sediment and the atmosphere. Glob. Biogeochem. Cycles https://doi.org/10.1029/2006gb002914.
Hedges, J.I., Eglinton, G., Hatcher, P.G., Kirchman, D.L., Arnosti, C., Derenne, S., Evershed, R.P., Kögel-Knabner, I., de Leeuw, J.W., Littke, R., Michaelis, W., Rullkötter, J., 2000. The molecularly-uncharacterized component of nonliving organic matter in natural environments. Org. Geochem. https://doi.org/10.1016/s0146-6380(00)00096-6.
Jones, M.W., Quine, T.A., de Rezende, C.E., Dittmar, T., Johnson, B., Manecki, M., Marques, J.S.J., de Aragão, L.E.O.C., 2017. Do regional aerosols contribute to the riverine export of dissolved black carbon? J. Geophys. Res. Biogeosci. https://doi.org/10.1002/2017jg004126.
Jönsson, A., Gustafsson, Ö., Axelman, J., Sundberg, H., 2003. Global accounting of PCBs in the continental shelf sediments. Environ.Sci.Technol. https://doi.org/10.1021/es0201404.
Jurado, E., Dachs, J., Duarte, C.M., Simó, R., 2008. Atmospheric deposition of organic and black carbon to the global oceans. Atmos. Environ. https://doi.org/10.1016/j.atmosenv.2008.07.029.
Kappenberg, A., Bläsing, M., Lehndorff, E., Amelung, W., 2016. Black carbon assessment using benzene polycarboxylic acids: limitations for organic-rich matrices. Org. Geochem. https://doi.org/10.1016/j.orggeochem.2016.01.009.
Kuehl, S.A., DeMaster, D.J., Nittrouer, C.A., 1986. Nature of sediment accumulation on the Amazon continental shelf. Cont. Shelf Res. https://doi.org/10.1016/0278-4343(86)90061-0.
Kuhlbusch, T.A.J., Crutzen, P.J., 1995. Toward a global estimate of black carbon in residues of vegetation fires representing a sink of atmospheric CO2 and a source of O2. Glob. Biogeochem. Cycles https://doi.org/10.1029/95gb02742.
Lara, L., Artaxo, P., Martinelli, L., Camargo, P., Victoria, R., Ferraz, E., 2005. Properties of aerosols from sugar-cane burning emissions in Southeastern Brazil. Atmos. Environ. https://doi.org/10.1016/j.atmosenv.2005.04.026.
Latrubesse, E.M., 2008. Patterns of anabranching channels: the ultimate end-member adjustment of mega rivers. Geomorphology https://doi.org/10.1016/j.geomorph.2008.05.035.
Laurance, W.F., Albernaz, A.K.M., Da Costa, C., 2001. Is deforestation accelerating in the Brazilian Amazon? Environ. Conserv. https://doi.org/10.1017/s0376892901000339.
Lian, F., Xing, B., 2017. Black carbon (biochar) in water/soil environments: molecular structure, sorption, stability, and potential risk. Environ.Sci.Technol. https://doi.org/10.1021/acs.est.7b02528.

Liu, J., Han, G., 2021. Tracing riverine particulate black carbon sources in Xijiang River basin: insight from stable isotopic composition and Bayesian mixing model. Water Res. https://doi.org/10.1016/j.watres.2021.116932.

Lohmann, R., Bollinger, K., Cantwell, M., Feichter, J., Fischer-Bruns, I., Zabel, M., 2009. Fluxes of soot black carbon to South Atlantic sediments. Glob. Biogeochem. Cycles https://doi.org/10.1029/2008gb003253.

Major, J., Lehmann, J., Rondon, M., Goodale, C., 2010. Fate of soil-applied black carbon: downward migration, leaching and soil respiration. Glob. Chang. Biol. https://doi.org/10.1111/j.1365-2486.2009.02044.x.

Malhi, Y., Wood, D., Baker, T.R., Wright, J., Phillips, O.L., Cochrane, T., Meir, P., Chave, J., Almeida, S., Arroyo, L., Higuchi, N., Killeen, T.J., Laurance, S.G., Laurance, W.F., Lewis, S.L., Monteagudo, A., Neill, D.A., Vargas, P.N., Pitman, N.C.A., Quesada, C.A., Salomão, R., Silva, J.N.M., Lezama, A.T., Terborgh, J., Martínez, R.V., Vinceti, B., 2006. The regional variation of aboveground live biomass in old-growth Amazonian forests. Glob. Chang. Biol. https://doi.org/10.1111/j.1365-2486.2006.01120.x.

Malhi, Y., Roberts, J.T., Betts, R.A., Killeen, T.J., Li, W., Nobre, C.A., 2008. Climate change, deforestation, and the fate of the Amazon. Science 319, 169–172. https://doi.org/10.1126/science.1146961.

Marchand, C., 2017. Soil carbon stocks and burial rates along a mangrove forest chronosequence (French Guiana). For. Ecol. Manag. https://doi.org/10.1016/j.foreco.2016.10.030.

Marchand, C., Lallier-Vergès, E., Baltzer, F., 2003. The composition of sedimentary organic matter in relation to the dynamic features of a mangrove-fringed coast in French Guiana. Estuar. Coast. Shelf Sci. https://doi.org/10.1016/s0272-7714(02)00134-8.

Marques, J.S.J., 2017. Carbono negro dissolvido no contínuo continente-oceano no rio Paraíba do Sul. Doctoral dissertation, Tese de doutoradoUniversidade Estadual do Norte Fluminense 2017.

Marques, J.S.J., Dittmar, T., Niggemann, J., Almeida, M.G., Gomez-Saez, G.V., Rezende, C.E., 2017. Dissolved black carbon in the headwaters-to-ocean continuum of Paraíba Do Sul River, Brazil. Front. Earth Sci. https://doi.org/10.3389/feart.2017.00011.

Martinelli, L.A., Nardoto, G.B., Soltangheisi, A., Reis, C.R.G., Abdalla-Filho, A.L., Camargo, P.B., Domingues, T.F., Faria, D., Figueira, A.M., Gomes, T.F., Lins, S.R.M., Mardegan, S.F., Mariano, E., Miatto, R.C., Moraes, R., Moreira, M.Z., Oliveira, R.S., Ometto, J.P.H., Santos, F.L.S., Sena-Souza, J., Silva, D.M.L., Silva, J.C.S., Vieira, S.A., 2021. Determining ecosystem functioning in Brazilian biomes through foliar carbon and nitrogen concentrations and stable isotope ratios. Biogeochemistry https://doi.org/10.1007/s10533-020-00714-2.

Masiello, C.A., 2004. New directions in black carbon organic geochemistry. Mar. Chem. https://doi.org/10.1016/j.marchem.2004.06.043.

Matos, C.R.L., Berrêdo, J.F., Machado, W., Sanders, C.J., Metzger, E., Cohen, M.C.L., 2020. Carbon and nutrient accumulation in tropical mangrove creeks, Amazon region. Mar. Geol. https://doi.org/10.1016/j.margeo.2020.106317.

McKee, B.A., Aller, R.C., Allison, M.A., Bianchi, T.S., Kineke, G.C., 2004. Transport and transformation of dissolved and particulate materials on continental margins influenced by major rivers: benthic boundary layer and seabed processes. Cont. Shelf Res. https://doi.org/10.1016/j.csr.2004.02.009.

Nakane, M., Ajioka, T., Yamashita, Y., 2017. Distribution and sources of dissolved black carbon in surface waters of the Chukchi Sea, Bering Sea, and the North Pacific Ocean. Front. Earth Sci. https://doi.org/10.3389/feart.2017.00034.

Nam, J.J., Gustafsson, O., Kurt-Karakus, P., Breivik, K., Steinnes, E., Jones, K.C., 2008. Relationships between organic matter, black carbon and persistent organic pollutants in European background soils: implications for sources and environmental fate. Environ. Pollut. https://doi.org/10.1016/j.envpol.2008.05.027.

Neupane, B., Wang, J., Kang, S., Zhang, Y., Chen, P., Rai, M., Guo, J., Yu, S., Thapa, P., 2020. Black carbon and mercury in the surface sediments of Selin Co, central Tibetan Plateau: covariation with total carbon. Sci. Total Environ. https://doi.org/10.1016/j.scitotenv.2020.137752.

Nittrouer, C.A., Curtin, T.B., DeMaster, D.J., 1986. Concentration and flux of suspended sediment on the Amazon continental shelf. Cont. Shelf Res. https://doi.org/10.1016/0278-4343(86)90058-0.

Oliveira, C.J., Clavier, J., 2000. Space-time variations of suspended material in the Sinnamary estuary, French Guiana: influence of Petit Saut electric dam. Rev. Bras. Oceanogr. https://doi.org/10.1590/S1413-77392000000100003.

Ometto, J.P.H.B., Ometto, J.P.H., Ehleringer, J.R., Domingues, T.F., Berry, J.A., Ishida, F.Y., Mazzi, E., Higuchi, N., Flanagan, L.B., Nardoto, G.B., Martinelli, L.A., 2006. The stable carbon and nitrogen isotopic composition of vegetation in tropical forests of the Amazon Basin, Brazil. Nitrogen Cycling in the Americas: Natural and Anthropogenic Influences and Controls https://doi.org/10.1007/978-1-4020-5517-1_12.

Ovalle, A.R.C., Silva, C.F., Rezende, C.E., Gatts, C.E.N., Suzuki, M.S., Figueiredo, R.O., 2013. Long-term trends in hydrochemistry in the Paraíba do Sul River, south-eastern Brazil. J. Hydrol. https://doi.org/10.1016/j.jhydrol.2012.12.036.

Parnell, A.C., Inger, R., Bearhop, S., Jackson, A.L., 2010. Source partitioning using stable isotopes: coping with too much variation. PLoS One 5, e9672. https://doi.org/10.1371/journal.pone.0009672.

Ray, R., Michaud, E., Aller, R.C., Vantrepotte, V., Gleixner, G., Walcker, R., Devesa, J., Le Goff, M., Morvan, S., Thouzeau, G., 2018. The sources and distribution of carbon (DOC, POC, DIC) in a mangrove dominated estuary (French Guiana, South America). Biogeochemistry https://doi.org/10.1007/s10533-018-0447-9.

RC Team, 2018. R: A Language And Environment for Statistical Computing. 2018R Foundation for Statistical Computing, Vienna, Austria.

Regnier, P., Friedlingstein, P., Ciais, P., Mackenzie, F.T., Gruber, N., Janssens, I.A., Laruelle, G.G., Lauerwald, R., Luyssaert, S., Andersson, A.J., Arndt, S., Arnosti, C., Borges, A.V., Dale, A.W., Gallego-Sala, A., Goddéris, Y., Goossens, N., Hartmann, J., Heinze, C., Ilyina, T., Joos, F., LaRowe, D.E., Leifeld, J., Meysman, F.J.R., Munhoven, G., Raymond, P.A., Spahni, R., Suntharalingam, P., Thullner, M., 2013. Anthropogenic perturbation of the carbon fluxes from land to ocean. Nat. Geosci. https://doi.org/10.1038/ngeo1830.

Reisser, M., Purves, R.S., Schmidt, M.W.I., Abiven, S., 2016. Pyrogenic carbon in soils: a literature-based inventory and a global estimation of its content in soil organic carbon and stocks. Front. Earth Sci. https://doi.org/10.3389/feart.2016.00080.

Rezende, C.L., Scarano, F.R., Assad, E.D., Joly, C.A., Metzger, J.P., Strassburg, B.B.N., Tabarelli, M., Fonseca, G.A., Mittermeier, R.A., 2018. From hotspot to hopespot: an opportunity for the Brazilian Atlantic Forest. Perspect. Ecol. Conserv. https://doi.org/10.1016/j.pecon.2018.10.002.

Ribas, L.M., 2012. Caracterização de fontes de matéria orgânica do estuário do rio Paraíba do Sul, RJ, Brasil. Doctoral dissertation, Tese de doutoradoUniversidade Estadual do Norte Fluminense 2012. Tese 131 pp.

Ribeiro, M.C., Metzger, J.P., Martensen, A.C., Ponzoni, F.J., Hirota, M.M., 2009. The Brazilian Atlantic Forest: how much is left, and how is the remaining forest distributed? Implications for conservation. Biol. Conserv. https://doi.org/10.1016/j.biocon.2009.02.021.

Richard, S., Arnoux, A., Cerdan, P., Reynouard, C., Horeau, V., 2000. Mercury levels of soils, sediments and fish in French Guiana, South America. Water Air Soil Pollut. 124 (3), 221–244. https://doi.org/10.1023/A:1005251016314.

Richey, J.E., Meade, R.H., Salati, E., Devol, A.H., Nordin, C.F., Dos Santos, U., 1986. Water discharge and suspended sediment concentrations in the Amazon River: 1982–1984. Water Resour. Res. https://doi.org/10.1029/wr022i005p00756.

Saiz, G., Wynn, J.G., Wurster, C.M., Goodrick, I., Nelson, P.N., Bird, M.I., 2015. Pyrogenic carbon from tropical savanna burning: production and stable isotope composition. Biogeosciences https://doi.org/10.5194/bg-12-1849-2015.

Sánchez-García, L., de Andrés, J.R., Gélinas, Y., Schmidt, M.W.I., Louchouarn, P., 2013. Different pools of black carbon in sediments from the Gulf of Cádiz (SW Spain): method comparison and spatial distribution. Mar. Chem. https://doi.org/10.1016/j.marchem.2013.02.006.

Schneider, M.P.W., Smittenberg, R.H., Dittmar, T., Schmidt, M.W.I., 2011. Comparison of gas with liquid chromatography for the determination of benzenepolycarboxylic acids as molecular tracers of black carbon. Org. Geochem. https://doi.org/10.1016/j.orggeochem.2011.01.003.

Shultz, D.J., Calder, J.A., 1976. Organic carbon variations in estuarine sediments. Geochim. Cosmochim. Acta https://doi.org/10.1016/0016-7037(76)90002-8.

Silva, M.A.L., Calasans, C.F., Ovalle, A.R.C., Rezende, C.E., 2001. Dissolved nitrogen and phosphorus dynamics in the lower portion of the Paraiba do Sul River, Campos dos Goytacazes, RJ, Brazil. Braz. Arch. Biol. Technol. https://doi.org/10.1590/s1516-89132001000400006.

Singh, N., Abiven, S., Torn, M.S., Schmidt, M.W.I., 2012. Fire-derived organic carbon in soil turns over on a centennial scale. Biogeosciences https://doi.org/10.5194/bg-9-2847-2012.

Smith, H.G., Sheridan, G.J., Lane, P.N.J., Nyman, P., Haydon, S., 2011. Wildfire effects on water quality in forest catchments: a review with implications for water supply. J. Hydrol. https://doi.org/10.1016/j.jhydrol.2010.10.043.

Sobrinho, R.de L., de L. Sobrinho, R., Bernardes, M.C., de Rezende, C.E., Kim, J.-H., Schouten, S., Sinninghe Damsté, J.S., 2021. A multiproxy approach to characterize the sedimentation of organic carbon in the Amazon continental shelf. Mar. Chem. https://doi.org/10.1016/j.marchem.2021.103961.

Solórzano, A., de Assis Brasil, L.S.C., de Oliveira, R.R., 2021. The Atlantic Forest ecological history: from pre-colonial times to the Anthropocene. The Atlantic Forest https://doi.org/10.1007/978-3-030-55322-7_2.

Souza, T.A., Godoy, J.M., Godoy, M.L.D., Moreira, I., Carvalho, Z.L., Salomão, M.S.M., Rezende, C.E., 2010. Use of multitracers for the study of water mixing in the Paraíba do Sul River estuary. J. Environ. Radioact. https://doi.org/10.1016/j.jenvrad.2009.11.001.

Stahl, C., Freycon, V., Fontaine, S., Dezécache, C., Ponchant, L., Picon-Cochard, C., Klumpp, K., Soussana, J.-F., Blanfort, V., 2016. Soil carbon stocks after conversion of Amazonian tropical forest to grazed pasture: importance of deep soil layers. Reg. Environ. Chang. https://doi.org/10.1007/s10113-016-0936-0.

Stock, B.C., Semmens, B.X., 2016. MixSIAR GUI User Manual. Version 3.1. https://doi.org/10.5281/zenodo.1209993.

Stock, B.C., Jackson, A.L., Ward, E.J., Parnell, A.C., Phillips, D.L., Semmens, B.X., 2018. Analyzing mixing systems using a new generation of Bayesian tracer mixing models. https://doi.org/10.7287/peerj.preprints.26884v1.

Stubbins, A., Spencer, R.G.M., Mann, P.J., Max Holmes, R., McClelland, J.W., Niggemann, J., Dittmar, T., 2015. Utilizing colored dissolved organic matter to derive dissolved black carbon export by arctic rivers. Front. Earth Sci. https://doi.org/10.3389/feart.2015.00063.

Sun, S., Schefuß, E., Mulitza, S., Chiessi, C.M., Sawakuchi, A.O., Zabel, M., Baker, P.A., Hefter, J., Mollenhauer, G., 2017. Origin and processing of terrestrial organic carbon in the Amazon system: lignin phenols in river, shelf, and fan sediments. Biogeosciences https://doi.org/10.5194/bg-14-2495-2017.

van der Werf, G.R., van der Werf, G.R., Randerson, J.T., Giglio, L., van Leeuwen, T.T., Chen, Y., Rogers, B.M., Mu, M., van Marle, M.J.E., Morton, D.C., James Collatz, G., Yokelson, R.J., Kasibhatla, P.S., 2017. Global fire emissions estimates during 1997–2016. Earth Syst.Sci.Data https://doi.org/10.5194/essd-9-697-2017.

Venables, W.N., Ripley, B.D., 2002. Modern applied statistics with S. Stat. Comput. https://doi.org/10.1007/978-0-387-21706-2.

Vitorello, V.A., Cerri, C.C., Andreux, F., Feller, C., Victória, R.L., 1989. Organic matter and natural Carbon-13 distribution in forested and cultivated oxisols. Soil Sci. Soc. Am. J. https://doi.org/10.2136/sssaj1989.03615995005300030024x.

Vuorio, K., Meili, M., Sarvala, J., 2006. Taxon-specific variation in the stable isotopic signatures (δ13C and δ15N) of lake phytoplankton. Freshw. Biol. https://doi.org/10.1111/j.1365-2427.2006.01529.x.

Wagner, S., Cawley, K.M., Rosario-Ortiz, F.L., Jaffé, R., 2015. In-stream sources and links between particulate and dissolved black carbon following a wildfire. Biogeochemistry https://doi.org/10.1007/s10533-015-0088-1.

Wagner, S., Jaffé, R., Stubbins, A., 2018. Dissolved black carbon in aquatic ecosystems. Limnol. Oceanogr. Lett. https://doi.org/10.1002/lol2.10076.

Wagner, S., Coppola, A.I., Stubbins, A., Dittmar, T., Niggemann, J., Drake, T.W., Seidel, M., Spencer, R.G.M., Bao, H., 2021. Questions remain about the biolability of dissolved black carbon along the combustion continuum. Nat. Commun. https://doi.org/10.1038/s41467-021-24477-y.

Wanderley, C.V.A., Godoy, J.M., Godoy, M.L.D., Rezende, C.E., Lacerda, L.D., Moreira, I., Carvalho, Z.L., 2013. Evaluating sedimentation rates in the estuary and shelf region of the Paraíba do Sul River, southeastern Brazil. J. Braz. Chem. Soc. https://doi.org/10.5935/0103-5053.20130268.

Ward, N.D., Krusche, A.V., Sawakuchi, H.O., Brito, D.C., Cunha, A.C., Moura, J.M.S., da Silva, R., Yager, P.L., Keil, R.G., Richey, J.E., 2015. The compositional evolution of dissolved and particulate organic matter along the lower Amazon River—Óbidos to the ocean. Mar. Chem. https://doi.org/10.1016/j.marchem.2015.06.013.

Wells, J.T., Coleman, J.M., 1981. Periodic mudflat progradation, northeastern coast of South America; a hypothesis. J. Sediment. Res. https://doi.org/10.2110/jsr.51.1069.

Wilkinson, B.H., McElroy, B.J., 2007. The impact of humans on continental erosion and sedimentation. Geol. Soc. Am. Bull. https://doi.org/10.1130/b25899.

Wolf, M., Lehndorff, E., Wiesenberg, G.L.B., Stockhausen, M., Schwark, L., Amelung, W., 2013. Towards reconstruction of past fire regimes from geochemical analysis of charcoal. Org. Geochem. https://doi.org/10.1016/j.orggeochem.2012.11.002.